LANGMUIR

pubs.acs.org/Langmuir Article

Nafion-Based Nanocarriers for Fluorine Magnetic Resonance Imaging

Marta Szczęch, Natalia Łopuszyńska, Wiktoria Tomal, Krzysztof Jasiński, Władysław P. Węglarz, Piotr Warszyński, and Krzysztof Szczepanowicz*

Cite This: *Langmuir* 2020, 36, 9534–9539

Read Online

ACCESS | Metrics & More | Article Recommendations

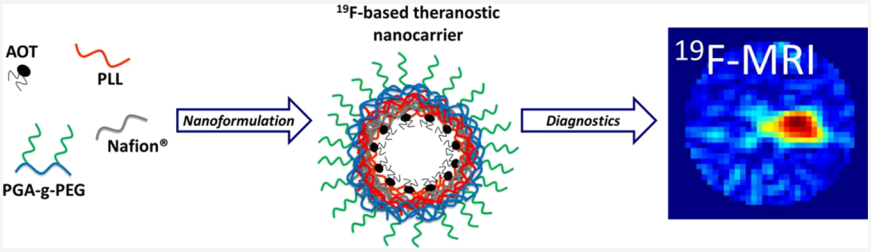

ABSTRACT: The aim of our study was to develop a novel method for nanocarriers' preparation as a fluorine magnetic resonance imaging (^{19}F MRI)-detectable drug delivery system. The novelty of the proposed approach is based on the application of fluorinated polyelectrolyte Nafion as a contrast agent since typical MRI contrast agents are based on paramagnetic gadolinium or ferro/superparamagnetic iron oxide compounds. An advantage of using an ^{19}F-based tracer comes from the fact that the ^{19}F image is detected at a different resonance frequency than the ^{1}H image. In addition, the close to zero natural concentration of ^{19}F nuclei in the human body makes fluorine atoms a promising MRI marker without any natural background signal. That creates the opportunity to localize and identify only exogenous fluorinated compounds with 100% specificity. The nanocarriers were formed by the deposition of polyelectrolytes on nanoemulsion droplets via the layer-by-layer technique with the saturation approach. The polyelectrolyte multilayer shell was composed of Nafion, the fluorinated ionic polymer used for labeling by ^{19}F nuclei, and poly-L-lysine (PLL). The surface of such prepared nanocarriers was further pegylated by adsorption of pegylated polyanion, poly-L-glutamic acid (PGA). The ^{19}F MRI-detectable hydrophobic nanocarriers with an average size of 170 nm and a sufficient signal-to-noise ratio have been developed and optimized to be used for passive tumor targeting and drug delivery.

INTRODUCTION

Nafion, developed by the DuPont in the late 1960s, is a sulfonated tetrafluoroethylene-based fluoropolymer-copolymer produced by copolymerization of a perfluorinated vinyl ether comonomer with tetrafluoroethylene, resulting in the Teflon-like backbone bearing hydrophilic sulfonic acid groups.[1] Nafion was the first synthetic polymer ever developed with ionic properties, and it started an entirely new class of polymers called ionomers.[2] It combines the physical and chemical properties of its Teflon base material with ionic characteristics, which results in specific properties: resistance to chemicals, relatively high working temperatures compared to other polymers, high ion conductivity (a cation exchange polymer), and very selective and high permeability for water. Nafion has initially been developed for use in separation membranes for chlor-alkali cells, but its properties make Nafion suitable for a broad range of applications like ion-exchange membranes, fuel cells, electrochemical devices, sensors, gas drying or humidification, and catalysis.[3−5] Biocompatibility studies on Nafion have shown no acute or chronic foreign body response,[6] which makes it one of the preferred systems capable of operating in harsh biological environments.[7,8] It has been applied as the material for biosensors, for controlled drug release, and for the formation of antimicrobial coatings.[8−11] Since Nafion possesses ^{19}F nuclei, it can also be used for fluorine magnetic resonance imaging (^{19}F MRI). Typical MRI contrast agents are based on paramagnetic gadolinium or ferro/superparamagnetic iron oxide compounds, producing positive or negative contrast in the ^{1}H MR image[12−14] due to the change of relaxation times T_1 or T_2 (T_2*) caused by local disturbances of the magnetic field experienced by water molecules in the imaged object in the surrounding of the contrast agent. Thus, the observed contrast

Received: May 21, 2020
Revised: July 24, 2020
Published: July 24, 2020

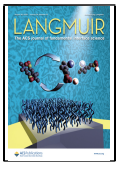

https://dx.doi.org/10.1021/acs.langmuir.0c01512
Langmuir 2020, 36, 9534−9539

change in the ^{1}H MR image is not specific to the presence of the magnetic tracer. A potential advantage of using an ^{19}F-based tracer comes from the fact that the ^{19}F image is detected at a different resonance frequency than the ^{1}H image.[15,16] In addition, the close to zero natural concentration of ^{19}F nuclei in the human body makes fluorine atoms a promising MRI marker without any natural background signal.[17] That creates the opportunity to localize and identify only exogenous fluorinated compounds with 100% specificity.

^{19}F MRI requires the use of fluorinated contrast agents, and the currently known can be divided into four groups: molecular tracers (small fluorinated molecules, e.g., hexafluorobenzene, perfluorodecalin, perfluorononane, perfluorooctyl bromide, perfluoro-15-crown-5-ether, and tetra(perfluoro-*tert*-butyl)pentaerythritol), polymers (linear fluorinated polymers, e.g., perfluoropolyether, 2,2,2-trifluoroethyl methacrylate, and 2-(dimethylamino)ethyl methacrylate), (hyper)branched derivatives (branched probes with several perfluorinated groups on their surface, e.g., ^{19}FIT), and inorganic nanoparticles functionalized with fluorinated ligands. Several methods of incorporation of fluorinated contrast agents into the nanoparticulate system like micelles, dendrimers, nanoemulsions, or inorganic nanoparticles have been described.[15,18−20]

Based on the data mentioned above, the present study aimed to develop a new strategy for the preparation of nanocarriers as an ^{19}F MRI-detectable drug delivery system. These nanocarriers were formed via the layer-by-layer technique deposition of polyelectrolyte shells on nanoemulsion drops. For that purpose, Nafion, the fluorinated anionic polymer used for labeling of formed nanocarriers by ^{19}F nuclei, was deposited together with a polycation, poly-L-lysine. Synthesized nanocarriers were further optimized for passive targeting to the tumors by pegylation of their surface.[21−26] These MRI-detectable nanocarriers for delivering a hydrophobic cargo can serve as an efficient contrast agent for ^{19}F MRI.

EXPERIMENTAL SECTION

Chemicals. The polycation poly-L-lysine (PLL) hydrobromide (M_w = 15−30 kDa) and polyanion, Nafion (663492) as well as chloroform, sodium chloride, and docusate sodium salt (AOT), were purchased from Sigma-Aldrich. All materials were used as received without further purification. A pegylated polyelectrolyte referred to as PGA-*g*-PEG was previously synthesized in our lab,[27] i.e., by coupling PEG (M_w = 5 kDa) chains to the PGA (M_w = 15−50 kDa) backbone (coupling rate ∼33%). Ultrapure water was produced using a Millipore Direct-Q5 UV purification system.

Nanocarrier Preparation and Characterization. Polyelectrolyte shell−liquid core nanocarriers were prepared according to the procedure proposed by us before,[27,28] i.e., by the encapsulation of nanoemulsion droplets in a polyelectrolyte multilayer shell. The oil phase for the nanoemulsification was prepared by dissolving an anionic surfactant, AOT, in chloroform at a concentration of 340 g/L, while the water phase was prepared by dissolving poly-L-lysine in 0.015 M NaCl solution (concentration varied from 10 to 300 ppm). The liquid cores of capsules (nanoemulsion droplets) were formed by dispersing the oil phase (0.1 mL) into the water phase (200 mL of polycation solution) during mixing with a magnetic stirrer at a rate of 300 rpm. On such prepared liquid cores, a multilayer shell was formed by the method of subsequent adsorption of polyelectrolytes (called the layer by layer).[29−31] PLL was used as a cationic polyelectrolyte and Nafion as an anionic one. To create pegylated nanocarriers, the surface of positively charged ones (with PLL as a top layer) was coated with the pegylated polyelectrolyte, PGA-*g*-PEG, using the same procedure as for the regular polyelectrolytes. As a result, pegylated polyelectrolyte shell−liquid core nanocarriers were prepared. After preparation, chloroform was evaporated to reach its final concentration, not exceeding 0.04 mg/L.[32] All synthesized nanocarriers were characterized by measuring their size, size distribution, zeta potential, concentration, and by morphology observation. As a final proof of potential application as an MRI-detectable drug delivery system, the prepared nanocarriers were imaged using ^{19}F MRI.

Experimental Techniques. *Dynamic Light Scattering (DLS).* Measurements were carried out with a Zetasizer Nano ZS instrument (Malvern-Pananalytical, UK) to determine the hydrodynamic diameter of nanocarriers. The measurements were performed at 25 °C in 0.015 M NaCl.

Laser Doppler Velocimetry (LDV). Methods were carried out with the Zetasizer Nano ZS instrument (Malvern-Pananalytical, UK) to determine the zeta potential of nanocarriers. The measurements were performed at 25 °C in 0.015 M NaCl.

Nanoparticle Tracking Analysis (NTA). The NTA technique with a NS500 instrument (NanoSight) was applied to determine the nanocarriers' concentration. The measurements were performed at 25 °C in 0.015 M NaCl.

Scanning Cryo-Electron microscopy (Cryo-SEM). Cryo-SEM was carried out using a Jeol JSM 7600F field emission scanning electron microscope (Jeol Ltd., Tokyo, Japan). The sample preparation and its imaging were performed according to the protocol described previously.[33] A droplet of a nanocarrier suspension was placed on a cold holder; then, the holder was immersed in liquid nitrogen slush using the Quorum PPT2000 cryo-preparation stage (Polaron, Quorum Technologies, United Kingdom). The frozen sample with the holder was raised and cryo-transferred at the temperature of liquid nitrogen vapors to the chamber of the cryo-unit where the sample was subjected to sublimation at −70 °C for 15−30 min. The sample was then sputter-coated with platinum (5 nm thickness). Following the coating, the specimen was transferred to the cooled stage of the microscope.

Quartz Crystal Microbalance (QCM). Analysis of the PLL/Nafion multilayer film formation and its pegylation was studied in situ using QCM-D (QSense AB Gothenburg, Sweden, present name: Biolin Scientific) at 25 °C. The sample preparation, handling, and analysis were performed according to the protocol described previously.[33] Sequential adsorption of polyelectrolytes was performed on quartz sensors coated with gold electrodes, having a fundamental resonance frequency of 4.95 MHz. After resonance frequency calibration, the chamber was filled up with the 0.015 M NaCl buffer to obtain a baseline. Then, the first polyelectrolyte, PLL (0.1 g/L), was introduced into the cell and the polymer adsorption kinetics was monitored in situ. After obtaining a constant value of resonance frequency, the chamber was rinsed with 0.015 M NaCl. Next, the analogous deposition procedure with the Nafion (negatively charged polyelectrolyte) followed by rinsing was carried out. The whole procedure was repeated until the required number of layers was obtained. The PLL-terminated film consisting of nine polyelectrolyte layers was pegylated by the deposition of PGA-*g*-PEG using the same procedure as for regular polyelectrolytes. The mass of adsorbed polyelectrolytes was calculated with the Sauerbrey equation.

Magnetic Resonance Imaging. ^{1}H and ^{19}F 3D ultrashort echo time (3D UTE) imagings of a gel phantom containing Nafion-loaded nanocarriers were performed at a 9.4 T Bruker Biospec 94/20 research MRI scanner with a 210 mm bore diameter and a high-performance actively shielded BGA 12S HP gradient system (675 mT/m) with integrated shims. A small transmit−receive RF ribbon solenoid coil (ID of 14 mm), which can be tuned either to ^{1}H or ^{19}F resonant frequency (i.e., 400.130 vs 376.498 MHz), was used for all experiments. The coil geometry was adjusted to the analyzed the sample size and shape to maximize SNR values.

3D UTE imaging of a phantom containing theranostic carriers was performed with the following imaging parameters: TR, 8 ms; TE, 0.16 ms; FA, 6.4°; RF pulse BW, 4.27 kHz; FOV, 4.0 × 4.0 × 4.0 cm. For ^{1}H images, MTX, 128 × 128 × 128; NA, 1; and acquisition time, ∼6 m 51 s were used, while for ^{19}F images, MTX, 32 × 32 × 32; NA, 256; and acquisition time, ∼1 h and 48 min were used.

https://dx.doi.org/10.1021/acs.langmuir.0c01512
Langmuir 2020, 36, 9534−9539

RESULTS AND DISCUSSION

In our previous works, we demonstrated embedding of iron oxide nanoparticles and gadolinium-based compounds into a polyelectrolyte shell as effective contrast agents for ^{1}H MR imaging, allowing visualization of the distribution of theranostic nanocapsules.[34,35] Here, we focused on the possibility of using a compound containing ^{19}F nuclei as an MRI agent. From the list of available fluorinated compounds, Nafion (fluorinated ionic polymer) seems to be the most promising to be used to label so-formed nanocarriers by ^{19}F nuclei. Since Nafion is not a commonly used polymer for the formation of multilayer films, therefore, to confirm the formation of the PLL/Nafion film and its pegylation by adsorption of pegylated polyelectrolyte PGA-*g*-PEG, quartz crystal microbalance (QCM) measurements were performed.

Changes in the oscillation resonance frequency, Δf, of the QCM crystal are related to the changes of adsorbed mass; a negative frequency shift is induced by the mass increase due to polyelectrolyte adsorption.[33] During the formation of the PLL/Nafion film and its pegylation, the frequency was downshifted with the number of deposited layers, as illustrated in Figure 1a. That indicated the growth of the multilayer film and its subsequent pegylation. To calculate mass as a function of the number of deposited layers, the Sauerbrey equation, implemented in the Q-Tools3 software (QSense), was applied (Figure 1b). The results show that the growth of the film mass is linear for the PLL/Nafion deposition, which is in agreement with the limited data available in the literature concerning the growth mode previously observed for other pairs of polycation/Nafion.[9,10] However, the polymer mass increment during the deposition step was higher for the Nafion layer than for the PLL one.

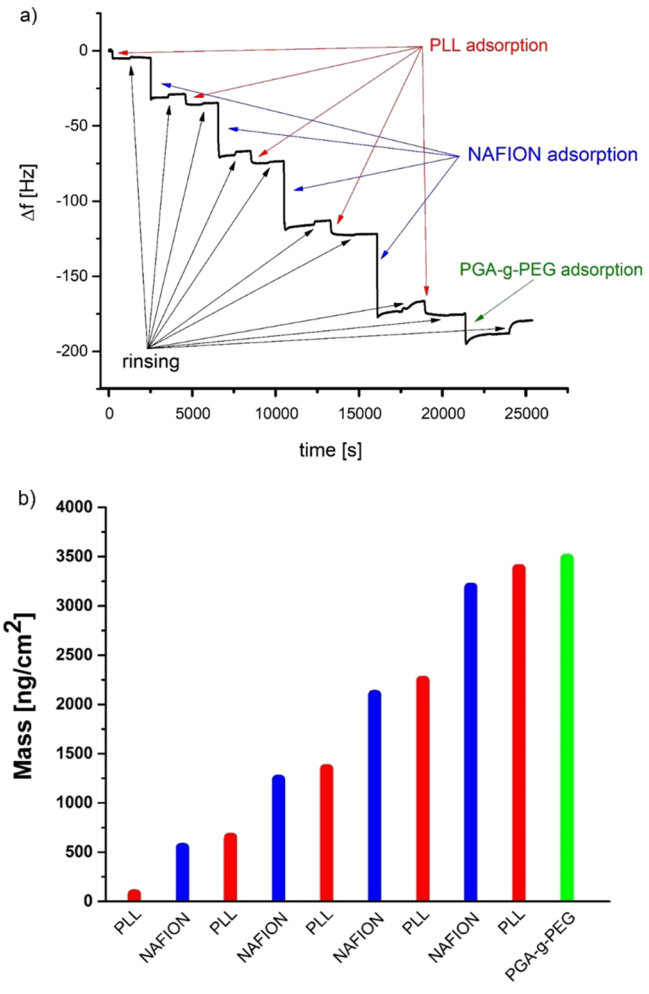

Figure 1. Quartz crystal microbalance (QCM) analysis, (a) frequency changes during film deposition, and (b) mass (per unit area) of PLL/Nafion films adsorbed at the QCM crystal and calculated using the Sauerbrey equation.

The QCM measurements confirmed the formation of the PLL/Nafion film and its pegylation; therefore, such a system (PLL, Nafion, and pegylated PGA) was used for nanocarrier preparation. They were prepared according to the procedure proposed before,[27] i.e., by the encapsulation of nanoemulsion droplets in the polymeric multilayer shell using the layer-by-layer technique. The nanoemulsion stabilized by the surfactant/polyelectrolyte interfacial complex was made by dispersing the oil phase (0.1 mL of chloroform containing an anionic surfactant, AOT) into the water phase (200 mL of PLL solution) during mixing with a magnetic stirrer (300 rpm). To minimize the presence of free, nonadsorbed polycation in prepared nanoemulsion, the concentration of PLL was varied from 50 to 300 ppm and the optimal conditions were determined by measuring the zeta potential of nanoemulsion droplets and by investigating their stability. This optimal amount of PLL corresponded to the point just before reaching a plateau of the zeta potential dependence versus the concentration of PLL, as shown in Figure 2a. The average size of prepared nanodroplets was 90 nm with a polydispersity index (PDI) below 0.2, and the zeta potential was equal to +68 ± 5 mV. For the preparation of drug-loaded nanocarriers, the oil phase also should contain selected drugs.[33,36] Those positively charged nanoemulsion cores were further encapsulated using the layer-by-layer technique and the saturation method with Nafion (concentration, 20 g/L) and PLL (concentration, 2 g/L) polyelectrolytes. To form the second polyanionic layer, a fixed volume of nanoemulsion cores was added to the Nafion solution during mixing with a magnetic stirrer at a rate of 300 rpm. The volume of the Nafion solution used to form a stable anionic layer was chosen empirically, analyzing the results of zeta potential measurements. Here, similar to the optimization of PLL addition, the optimal amount of Nafion corresponded to the point just before reaching the plateau of the zeta potential dependence on the concentration of Nafion (cf., Figure 2b). Consequently, the presence of free, unadsorbed Nafion in the nanocarrier suspension was minimized as most of it were used to form the Nafion layer and to reverse nanocarriers' charge. The next layers in the PLL/Nafion multilayer shell were formed by repeating the procedure described above. A typical saw-like pattern of the dependence of the zeta potential of nanocarriers on the adsorption of subsequent layers, as depicted in Figure 3, is evidence of the formation of a multilayer shell. To create pegylated nanocarriers, the ones with a PLL-terminated shell (with deposited five polyelectrolyte layers) were coated with the layer of PGA-*g*-PEG using the same procedure as described above. As a result, we prepared pegylated polyelectrolyte shell−liquid core nanocarriers. The average size of those nanocarriers measured by the DLS method was ∼170 nm. That size was additionally confirmed by Cryo-SEM observation, as illustrated in Figure 4. The zeta potential of pegylated nanocarriers measured by the LDV method was ca. 0 mV (cf., Figure 4). The final nanocarrier concentration determined by

https://dx.doi.org/10.1021/acs.langmuir.0c01512
Langmuir 2020, 36, 9534−9539

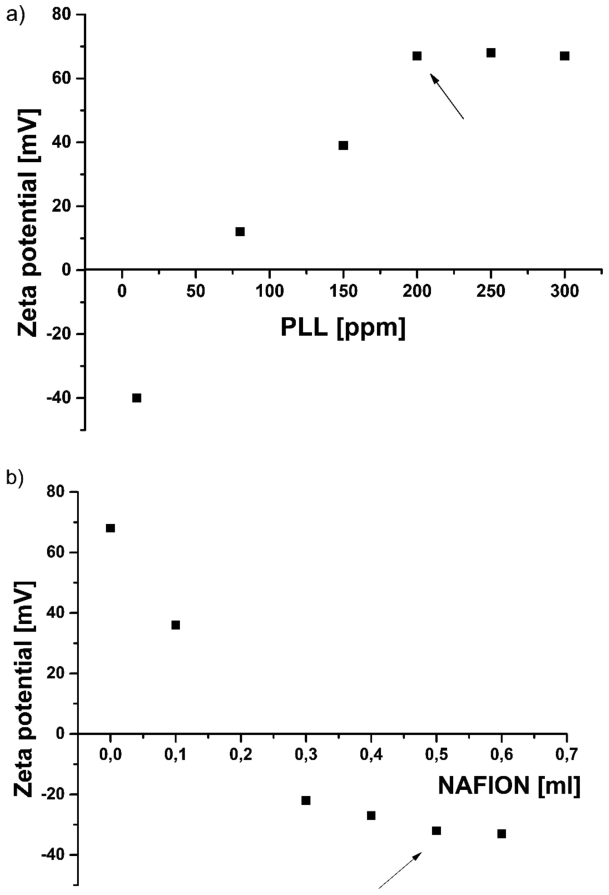

Figure 2. Example of determining the optimal polyelectrolyte concentration/amount: (a) dependence of the zeta potential of the nanoemulsion core on PLL concentration. (b) Dependence of the zeta potential of nanocarriers on the Nafion amount (the optimal concentration/amount of polyelectrolyte used to form a stable polyelectrolyte layer is pointed by an arrow).

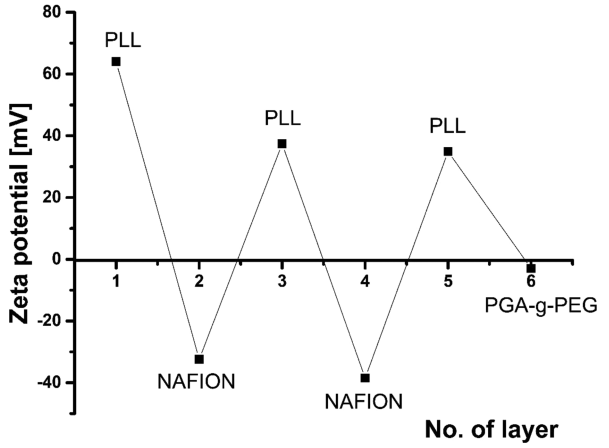

Figure 3. Saw-like pattern of the dependence of nanocarriers' zeta potential on the adsorption of subsequent layers.

NTA was ~1.5 × 10^{12} nanocarriers/mL. Properties of synthesized nanocarriers were optimized for biomedical applications as their size was in the range of optimum dimensions suggested for tumor-targeting nanocarriers (100–400 nm), which enables the leakage of the particles from the tumor vessels to the tumor tissue and ensures their efficient endocytosis by epithelial cells.[21,22] Since the surface of

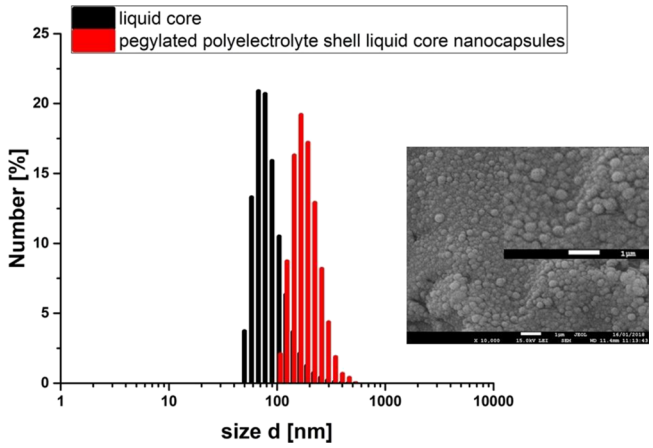

Figure 4. Average size of pegylated polyelectrolyte shell–liquid core nanocarriers measured by the DLS method and imaged by Cryo-SEM.

synthesized nanocarriers was functionalized by the pegylated polyelectrolyte, which resulted in the formation of PEG corona at nanocarriers' shell (protein-resistant layer), it provided the steric stabilization in the high salt conditions, essential for the biomedical applications and made them less visible to phagocytic cells.[37]

The ^{19}F MR imaging of an agar phantom containing nanocarriers with Nafion incorporated in one of the shell layers was performed to check the possibility of visualizing the distribution of theranostic carriers in samples. The results presented in Figure 5 shows MR images based on proton and fluorine resonances as well as an overlay of these two, which is a typical way to present the distribution of fluorine nuclei in the imaged tissue or organs. The visible outer limits of the fluorine image are somewhat smaller than for the hydrogen one. This is due to the smaller resolution of the fluorine image. For the curved sample geometry, thresholding above the noise level in each pixel leads to loss of some finer details, which are more clearly visible in the ^{1}H image. The corresponding number of ^{19}F nuclei per 1 mL of the sample, contributing to the image shown in Figure 5, was 2.8 × 10^{18}. The estimated signal-to-noise ratio (SNR) for the ^{19}F image was about 12 for indicated experimental conditions. Shortening the experimental time (TA) to less than 30 min, which is more relevant for *in vivo* conditions, decreases the SNR to about 5. Such an SNR was still high enough to reasonably visualize the distribution of fluorine in the sample. Thus, we directly confirmed the possibility of detecting Nafion-loaded theranostic nanocapsules using ^{19}F MRI. The obtained results for Nafion-based nanocarriers are comparable with that theoretically more known for application as ^{19}F MRI tracers; however, more investigation and further analysis is required.

CONCLUSIONS

We proposed a novel strategy for the preparation of theranostic nanocarriers based on ^{19}F MR imaging. The fluorinated ionic polymer, Nafion, was used to form the polymeric shell of nanocarriers as well as to provide the ^{19}F nuclei to formed nanocarriers. The synthesized nanocarriers were optimized for tumor passive targeting since their size is favorable to provide a sufficient level of target accumulation, and the pegylation of their surface may decrease fast clearance, thus prolonging their circulation. Proposed nanocarriers can, therefore, serve as efficient contrast agents that can be

https://dx.doi.org/10.1021/acs.langmuir.0c01512
Langmuir 2020, 36, 9534–9539

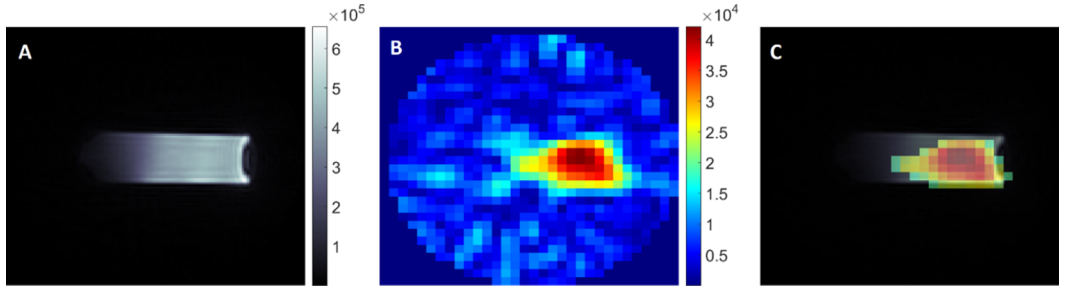

Figure 5. (A) ^{1}H MR Image of phantom containing nanocarriers (UTE3D; FOV, 4.0 cm; MTX, 128; NA, 1; TA, ∼7 min), (B) corresponding ^{19}F MR image (UTE3D; FOV, 4.0 cm; MTX, 32; NA, 256; TA, 1 h and 48 min), and (C) an overlay of ^{1}H and ^{19}F images.

observed/monitored by ^{19}F MRI and simultaneously deliver a hydrophobic cargo. The obtained results fulfill the first step of investigation for biomedical application of Nafion-based nanocarriers, which is mandatory for the planning of any *in vitro* and *in vivo* studies. Further work will be focused on bioanalysis, including biocompatibility, genotoxicity, localization (^{19}F MRI), etc.

AUTHOR INFORMATION

Corresponding Author

Krzysztof Szczepanowicz − *Institute of Catalysis and Surface Chemistry, Polish Academy of Sciences, Kraków 30-239, Poland;* orcid.org/0000-0002-9927-5869;
Phone: +48126395121; Email: ncszczep@cyf-kr.edu.pl;
Fax: +48124251923

Authors

Marta Szczęch − *Institute of Catalysis and Surface Chemistry, Polish Academy of Sciences, Kraków 30-239, Poland*

Natalia Łopuszyńska − *Institute of Nuclear Physics, Polish Academy of Sciences, Kraków 31-342, Poland*

Wiktoria Tomal − *Institute of Catalysis and Surface Chemistry, Polish Academy of Sciences, Kraków 30-239, Poland*

Krzysztof Jasiński − *Institute of Nuclear Physics, Polish Academy of Sciences, Kraków 31-342, Poland*

Władysław P. Węglarz − *Institute of Nuclear Physics, Polish Academy of Sciences, Kraków 31-342, Poland*

Piotr Warszyński − *Institute of Catalysis and Surface Chemistry, Polish Academy of Sciences, Kraków 30-239, Poland;* orcid.org/0000-0001-5449-9060

Complete contact information is available at: https://pubs.acs.org/10.1021/acs.langmuir.0c01512

Notes

The authors declare no competing financial interest.

ACKNOWLEDGMENTS

This research was funded in part by NCN Project OPUS UMO-2015/17/B/ST5/02808 and the statutory research fund of ICSC PAS. N.Ł. acknowledges the support of InterDokMed project no. POWR.03.02.00-00-I013/16.

REFERENCES

(1) Gardiner, J. Fluoropolymers: origin, production, and industrial and commercial applications. *Aust. J. Chem.* **2015**, *68*, 13−22.

(2) Perma Pure LLC (2004).*Technical Notes and Articles. Archived from on September 28, 2013.*

(3) Heitner-Wirguin, C. Recent advances in perfluorinated ionomer membranes: structure, properties and applications. *J. Membr. Sci.* **1996**, *120*, 1−33.

(4) Mauritz, K. A.; Moore, R. B. State of understanding of Nafion. *Chem. Rev.* **2004**, *104*, 4535−4586.

(5) Gelbard, G. Organic synthesis by catalysis with ion-exchange resins. *Ind. Eng. Chem. Res.* **2005**, *44*, 8468−8498.

(6) Turner, R. F. B.; Harrison, D. J.; Rojotte, R. V. Preliminary in vivo biocompatibility studies on perfluorosulphonic acid polymer membranes for biosensor applications. *Biomaterials* **1991**, *12*, 361−368.

(7) Wilkins, E.; Atanasov, P.; Muggenburg, B. A. Integrated implantable device for long-term glucose monitoring. *Biosens. Bioelectron.* **1995**, *10*, 485−494.

(8) Dai, Z.; Möhwald, H. Highly stable and biocompatible nafion-based capsules with controlled permeability for low-molecular-weight species. *Chem. − Eur. J.* **2002**, *8*, 4751−4755.

(9) Gibbons, E. N.; Winder, C.; Barron, E.; Fernandes, D.; Krysmann, M. J.; Kelarakis, A.; Parry, A. V. S.; Yeates, S. G. Layer by Layer Antimicrobial Coatings Based on Nafion, Lysozyme, and Chitosan. *Nanomaterials* **2019**, *9*, 1563.

(10) Yoshida, K.; Sato, K.; Ono, T.; Dairaku, T.; Kashiwagi, Y. Preparation of nafion/polycation layer-by-layer films for adsorption and release of insulin. *Polymer* **2018**, *10*, 812.

(11) Yi, Q.; Sukhorukov, G. B. Externally triggered dual function of complex microcapsules. *ACS Nano* **2013**, *7*, 8693−8705.

(12) Hingorani, D. V.; Bernstein, A. S.; Pagel, M. D. A review of responsive MRI contrast agents: 2005−2014. *Contrast Media Mol. Imaging* **2015**, *10*, 245−265.

(13) Runge, V. M.; Clanton, J. A.; Lukehart, C. M.; Partain, C. L.; James, A. E., Jr. Paramagnetic agents for contrast-enhanced NMR imaging: a review. *Am. J. Roentgenol.* **1983**, *141*, 1209−1215.

(14) Sun, C.; Lee, J. S. H.; Zhang, M. Magnetic nanoparticles in MR imaging and drug delivery. *Adv. Drug Delivery Rev.* **2008**, *60*, 1252−1265.

(15) Tirotta, I.; Dichiarante, V.; Pigliacelli, C.; Cavallo, G.; Terraneo, G.; Bombelli, F. B.; Metrangolo, P.; Resnati, G. ^{19}F magnetic resonance imaging (MRI): from design of materials to clinical applications. *Chem. Rev.* **2014**, *115*, 1106−1129.

(16) Ruiz-Cabello, J.; Barnett, B. P.; Bottomley, P. A.; Bulte, J. W. M. Fluorine (^{19}F) MRS and MRI in biomedicine. *NMR Biomed.* **2011**, *24*, 114−129.

(17) Costa, J. L.; Dobson, C. M.; Kirk, K. L.; Poulsen, F. M.; Valeri, C. R.; Vecchione, J. J. Studies of human platelets by ^{19}F and ^{31}P NMR. *FEBS Lett.* **1979**, *99*, 141−146.

(18) Knight, J. C.; Edwards, P. G.; Paisey, S. J. Fluorinated contrast agents for magnetic resonance imaging; a review of recent developments. *RSC Adv.* **2011**, *1*, 1415−1425.

(19) Celentano, W.; Neri, G.; Distante, F.; Li, M.; Messa, P.; Chirizzi, C.; Chaabane, L.; De Campo, F.; Metrangolo, P.; Bombelli, F. B.; Cellesi, F. Design of fluorinated hyperbranched polyether copolymers for ^{19}F MRI nanotheranostics. *Polym. Chem.* **2020**, *11*, 3951.

(20) Bouchoucha, M.; van Heeswijk, R. B.; Gossuin, Y.; Kleitz, F.; Fortin, M.-A. Fluorinated mesoporous silica nanoparticles for binuclear probes in ^{1}H and ^{19}F magnetic resonance imaging. *Langmuir* **2017**, *33*, 10531−10542.

https://dx.doi.org/10.1021/acs.langmuir.0c01512
Langmuir 2020, 36, 9534−9539

(21) Matsumura, Y.; Kataoka, K. Preclinical and clinical studies of anticancer agent-incorporating polymer micelles. *Cancer Sci.* **2009**, *100*, 572−579.
(22) Matsumura, Y.; Maeda, H. A New Concept for Macromolecular Therapeutics in Cancer Chemotherapy: Mechanism of Tumoritropic Accumulation of Proteins and the Antitumor Agent Smancs. *Cancer Res.* **1986**, *46*, 6387−6392.
(23) Monsky, W. L.; Fukumura, D.; Gohongi, T.; Ancukiewcz, M.; Weich, H. A.; Torchilin, V. P.; Yuan, F.; Jain, R. K. Augmentation of transvascular transport of macromolecules and nanoparticles in tumors using vascular endothelial growth factor. *Cancer Res.* **1999**, *59*, 4129−4135.
(24) Gref, R.; Minamitake, Y.; Peracchia, M. T.; Trubetskoy, V.; Torchilin, V.; Langer, R. Biodegradable long-circulating polymeric nanospheres. *Science* **1994**, *263*, 1600−1603.
(25) Torchilin, V. Nanopreparations for delivery of non-deliverable pharmaceuticals. *Am. Pharm. Rev.* **2013**, *16* ().
(26) Schäfer-Korting, M. Drug delivery. In *Passive and active drug targeting: drug delivery to tumors as an example*; Springer: 2010; pp. 3−53.
(27) Szczepanowicz, K.; Hoel, H. J.; Szyk-Warszynska, L.; Bielańska, E.; Bouzga, A. M.; Gaudernack, G.; Simon, C.; Warszynski, P. Formation of biocompatible nanocapsules with emulsion core and pegylated shell by polyelectrolyte multilayer adsorption. *Langmuir* **2010**, *26*, 12592−12597.
(28) Szczepanowicz, K.; Dronka-Góra, D.; Para, G.; Warszyński, P. Encapsulation of liquid cores by layer-by-layer adsorption of polyelectrolytes. *J. Microencapsulation* **2010**, *27*, 198−204.
(29) Sukhorukov, G. B.; Donath, E.; Lichtenfeld, H.; Knippel, E.; Knippel, M.; Budde, A.; Möhwald, H. Layer-by-layer self assembly of polyelectrolytes on colloidal particles. *Colloids Surf., A* **1998**, *137*, 253−266.
(30) Antipov, A. A.; Sukhorukov, G. B. Polyelectrolyte multilayer capsules as vehicles with tunable permeability. *Adv. Colloid Interface Sci.* **2004**, *111*, 49−61.
(31) Decher, G.; Schlenoff, J. B. *Multilayer thin films: sequential assembly of nanocomposite materials*; Wiley-VCH: 2003.
(32) Łukasiewicz, S.; Szczepanowicz, K. In vitro interaction of polyelectrolyte nanocapsules with model cells. *Langmuir* **2014**, *30*, 1100−1107.
(33) Szczepanowicz, K.; Bzowska, M.; Kruk, T.; Karabasz, A.; Bereta, J.; Warszynski, P. Pegylated polyelectrolyte nanoparticles containing paclitaxel as a promising candidate for drug carriers for passive targeting. *Colloids Surf., B* **2016**, *143*, 463−471.
(34) Szczęch, M.; Karabasz, A.; Łopuszyńska, N.; Bzowska, M.; Węglarz, W. P.; Warszyński, P.; Szczepanowicz, K. Gadolinium labeled polyelectrolyte nanocarriers for theranostic application. *Colloids Surf., B* **2019**, *183*, 110396.
(35) Szczepanowicz, K.; Piechota, P.; Węglarz, W. P.; Warszyński, P. Polyelectrolyte nanocapsules containing iron oxide nanoparticles as MRI detectable drug delivery system. *Colloids Surf.,A* **2017**, *532*, 351−356.
(36) Bzowska, M.; Karabasz, A.; Szczepanowicz, K. Encapsulation of camptothecin into pegylated polyelectrolyte nanocarriers. *Cooloids Surf., A* **2018**, *557*, 36−42.
(37) Łukasiewicz, S.; Szczepanowicz, K.; Błasiak, E.; Dziedzicka-Wasylewska, M. Biocompatible Polymeric Nanoparticles as Promising Candidates for Drug Delivery. *Langmuir* **2015**, *31*, 6415−6425.

https://dx.doi.org/10.1021/acs.langmuir.0c01512
Langmuir 2020, 36, 9534−9539